Random Vibration Peaks in Rotorcraft and the Effects of Nonuniform Gusts

G. H. Gaonkar*
Southern Illinois University, Edwardsville, Ill.

The analysis of random blade vibrations is extended 1) to include the average number of peaks above arbitrary thresholds, and 2) to the case of both longitudinally and laterally nonuniform or completely nonuniform vertical turbulence over the rotor disk. This extended analysis provides a means of assessing the validity of uniform and partially nonuniform (nonuniform only in the longitudinal direction) approximate turbulence models used earlier. Further, it exactly identifies threshold ranges above which peak distribution functions (PDF) over one rotor revolution can be approximated by the statistics of threshold upcrossings. This PDF over one revolution directly gives the probability that any maxima or peaks in one revolution are less than or equal to the required thresholds. For illustrative purposes, the selected problem refers to random flap bending at high advance ratios. The general turbulence theory includes cross correlation between inputs from different blade stations. In the numerical evaluation only one representative station at 0.7 radius is used. Numerical results demonstrate that the average number of threshold upcrossings and peaks per unit time differ significantly for all values of response levels and azimuth positions. Consequently, the approximation of PDF conditional on the occurrence of a peak at any instant by threshold upcrossing expectations is not satisfactory. Two other important findings are 1) the effects of nonuniform turbulence are negligible, justifying the previously made assumption according to which all parts of the rotor-disk experience at a given instant basically the same turbulence velocity, and 2) the formulation of approximating the PDF over one rotor revolution by corresponding threshold-crossing statistics is satisfactory for rotor applications. After having ascertained by the extended analysis the approximate validity of these two findings, the computation of vibration statistics in the linear range is no more involved than computing response histories to individual gusts.

Nomenclature

$\bar{t}$ = time, sec
Ω = angular rotor speed, rad/sec
$t = \Omega \bar{t}$ = dimensionless time
v = flight velocity, fps
R = rotor radius, ft
$\mu = v/\Omega R$ = rotor advance ratio
γ = rigid blade Lock inertia number
B = tip-loss factor
r = radius of blade station
$x = R/r$ = dimensionless radius of blade station
EI = flap-bending stiffness of blade
EI_0 = root stiffness of blade
η_h = first elastic mode of uniform hinged-free beam
χ = adaptation factor for first mode representation: $\eta = x + \chi\eta_h$
w = vertical turbulence velocity components
λ = $w/\Omega R$ {inflow ratio, or dimensionless vertical turbulence, (positive up)}
$\beta(t)$ = flapping angle
L = the scale length of the longitudinal turbulence component
c_k, c_ℓ = dimensionless constants ≤ 1
$\lambda_k(t)$ = inflow at blade station distant $c_k R$ from the rotor center (λ_k is identical to λ when $c_k = 0.7$)
$R_{k\ell}(t_1, t_2)$ = correlation functions of inflow at blade stations $c_k R$ and $c_\ell R$ from the rotor center (cross correlation if $c_k \neq c_\ell$, and autocorrelation if $c_k = c_\ell$)
$R_\lambda(t_1, t_2) = R_{kk}(t_1, t_2)$ with $c_k = 0.7$ = autocorrelation function of inflow at $0.7R$ blade station
$\sigma_\beta(t) = \sqrt{R_\beta(t,t)}$ = standard deviation of $\beta(t)$
$\sigma_{\beta\max}$ = maximum value of $\sigma_\beta(t)$ in one rotor revolution
$C_1(t), C_2(t)$ = aerodynamic damping function
$K_1(t), K_2(t)$ = aerodynamic stiffness function
$m_\lambda(t)$ = input modulating function (flap moment derivative)
p = flapping frequency
$P(t)$ = state or response variance matrix
ξ = threshold or response level
$E[N_{+\beta}(\xi, t)]$ = average number of flapping upcrossings (with positive slope) of threshold ξ per unit time
$E[M_\beta(\xi, t)]$ = average number of flapping peaks above ξ per unit time
$E[M_{\beta T}(t)] = E[M_\beta(-\infty, t)]$ = average number of flapping peaks per unit time irrespective of magnitude (average total peak rate)
$F_\beta(\xi, t)$ = distribution function of flapping peaks conditional on the occurrence of a peak at t
$\rho_\beta(\xi)$ = a parameter defining the average narrow-band features of flapping above ξ, Eq. (26)
$F_{\beta T}(\xi)$ = distribution function of flapping peaks over one rotor revolution, Eq. (27)

Received Aug. 11, 1975; revision received June 7, 1976.
Index categories: VTOL Vibration; Structural Dynamic Analysis.
*Research Professor & Coordinator. Member AIAA.

I. Introduction

ALTHOUGH the effects of turbulence on rotor vibrations and loads are not substantial in the normal helicopter

regimes, these effects become very important for unloaded rotors operating at high advance ratios.[1-5] Such rotors, in order to avoid flapping instability, must have blades with high flap-wise bending stiffness.[4,5] In spite of the use of stiff blades, good handling qualities can be obtained by suitable feedback systems.[5] This paper is concerned with analytical methods of computing the effects of atmospheric turbulence on unloaded rotors with stiff flap-wise blades at high advance ratios. As in Refs. 1 to 5, the induced flow from the turbulence excitation is neglected. In general, at conditions of low rotor-lift and high advance ratios ($\mu > 0.7$), typical of compound rotorcraft with rotor off-loading by a fixed wing, the induced flow effects will be negligible.[1-2,6]

With the exception of Refs. 7 and 8, rotor-gust for above conditions has been studied on the assumption that the vertical turbulence is uniform over the rotor disk. This means that the vertical turbulence at the rotor center is a representative sample for the entire disk. A less restrictive model is developed in Refs. 7 and 8, which includes the effects of nonuniformity of vertical turbulence only in the longitudinal or flight direction. The "lateral nonuniformity of the vertical turbulence velocity, because it is more elaborate to evaluate, has not been considered as yet."[8] In this paper, a generalized model of turbulence in the rotor plane is developed, which is advanced over the preceding ones in two respects: 1) it includes the nonuniformity of turbulence both in the lateral and longitudinal directions, from which earlier approximate models can be derived as special cases, 2) it permits cross correlation between inputs from different blade stations.

Mention must also be made of two other studies[9,10] in which the autocorrelation function of the inflow is expressed in terms of both time and space coordinates. These studies[9,10] are an application of an earlier basic study due to Wan[11] for the dynamic analysis of continua subject to generalized random loading. In the present paper, it is possible to use the well-established Taylor-von Karman theory. This theory is based on a "temporarily frozen" turbulence field such that measured time histories can be converted into space histories and vice-versa. Recent theoretical and experimental studies of Appa Rao[12] on propellers operating in turbulence also support this viewpoint. Therefore, a general theory of correlation functions comprising both time and space coordinates, as in Refs. 9, 10, and 11, is not required. Further elaboration for the approach taken in this paper is discussed in the next section.

In the case of uniform turbulence, the rotor-response variance matrix can be directly evaluated by using the shaping filter method.[13] Related computational aspects are no more involved than those used to generate response histories to step-gusts.[13] However, whether the nonuniformity is considered only in the flight direction or over the entire rotor disk, the gust inputs represent a nonstationary process modulated by periodic functions. For such nonstationary inputs, the method of shaping filters loses its simplicity.[13] Therefore it is of interest to assess the range of validity of approximate models based on uniform turbulence.

The analysis of the nonstationary random response processes are usually restricted to narrow-band processes.[14-16] Of particular importance are peak statistics which are readily analyzed for narrow-band random processes.[14-16] Blade response peak statistics have been developed in Refs. 15 and 16. In Ref. 15, peak statistics are studied on the basis of $E[N_+(\xi,t)]$, or the average number of upcrossings of threshold ξ per unit time, $\partial/\partial\xi E[N_+(\xi,t)]$, the probability density of peak magnitude conditional on the occurrence of a peak, and $E[M(-\infty,t)]$ or the average number of peaks per unit time irrespective of magnitude, for all of which closed form expressions are available.[15] Extensions in Ref. 16 include tortional flexibility and the probability density of peak magnitude over one rotor revolution. For lower level responses the narrow band features is not well realized.[15-16] In this paper, results of $E[M(\xi,t)]$, or average number of peaks per unit time above any threshold ξ are obtained numerically; and criteria for using the narrow-band approximation in determining the upper level peak distribution over one revolution are developed. The following peak statistics analysis thus provides an analytical basis for the narrow-band approximation, and the peak distribution function which directly gives the probability that any response peak in one rotor revolution is less than or equal to required thresholds.

For illustrative purposes, the problem of flap-bending of uniform and tapered-in-thickness blades is treated. The selected rotor parameters are representative of hingeless compound rotorcraft. The developed methods are also of interest to several other V/STOL configurations. For examples, in case of stowed rotors, the turbulence will have an appreciable effect on loads during folding and stowing operations.[1] The same is true of large diameter propellers in V/STOL and tilt-rotor airplanes.[12,17]

II. Nonuniform Turbulence in the Rotor Plane

In an exact description, atmospheric turbulence velocities are random functions of both time and space coordinates, similar to boundary-layer turbulence. In studies of gust response control and loads analysis, atmospheric turbulence is described on the basis of G. I. Taylor's hypothesis, according to which the gust field is momentarily frozen with respect to time.[7,18] In other words, the aircraft passes through the random waves of turbulence much like it rolls over a bumpy runway with randomly spaced parallel bumps. The reasoning is that the aircraft traverses through the eddies so fast that the turbulence relative to the aircraft can be treated as a random surface. The widely used von Karman turbulence model is based on this hypothesis. The assumptions and other analytical details employed to arrive at this model are rather numerous and are extensively discussed in the literature.[7,18] It should be noted that Taylor's hypothesis provides the feasibility of dual conversion, i.e., time histories of turbulence measured from the aircraft can be converted into spatial records and vice-versa. Thus, if x is the distance traveled by a point in the gust field relative to the aircraft in a time interval τ, then $x = v\tau$, where v is the mean flight speed. It is therefore possible to describe such statistical functions as the autocorrelation function either in terms of x or τ. Such a dual conversion is often not possible when the turbulence field is random in space and time.

We now present a generalized stochastic model of vertical turbulence in the rotor plane. For algebraic simplicity, we stipulate that the turbulence excitation has zero mean values. This model includes nonuniformity both in the lateral and longitudinal directions of the rotor disk and permits cross correlation between inputs from different blade stations. Our approach follows the Taylor-von Karman turbulence theory based on the concept of frozen random space waves. There are three reasons for this approach. First, for high advance ratio and low rotor-thrust conditions, self-induced turbulence in the rotor plane is likely to be negligible.[1,2,6] Therefore, the gust excitations on rotor blades are essentially due to free atmospheric turbulence, for which the applicability of frozen space wave concept is well established.[7] Second, the Taylor-von Karman theory agrees well with low altitude turbulence data.[19] Third, during high advance ratio flight regimes, the Taylor-von Karman turbulence theory is applicable, since the mean flow velocity relative to the rotorcraft is large compared with the turbulence velocities. For example, a standard deviation of 8 fps for the vertical turbulence velocities occurs with 0.1% probability at altitudes between 400 and 700 ft above terrain[19]; whereas for an unloaded rotor with an advance ratio of 1.6, the cruising speed is about 280 knots (480 fps) at a tip-speed of 300 fps. However, it should be noted that the Taylor-von Karman theory is not applicable to hovering conditions.[7]

As seen in Fig. 1, we select a coordinate system which moves with constant flight speed v and at the same time

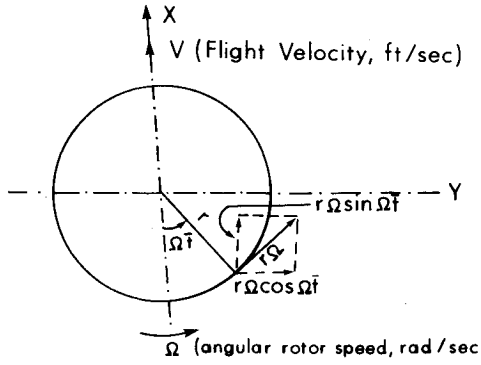

Fig. 1 Components of blade velocity at a blade station with radius r.

rotates with rotor angular velocity Ω. Consider two blade stations k and ℓ with coordinates $(x_k(\bar{t}), y_k(\bar{t}))$ and $(x_\ell(\bar{t}), y_\ell(\bar{t}))$. The cross correlation function between vertical turbulence velocities $w(\bar{t}_1)$ and $w(\bar{t}_2)$, respectively, at stations k and ℓ is given by

$$R_{k\ell}(\bar{t}_1,\bar{t}_2) = E[w(x_k(\bar{t}_1), y_k(\bar{t}_1))\, w(x_\ell(\bar{t}_2), y_\ell(\bar{t}_2))] \tag{1}$$

where E represents the expectation or averaging operation. Using G. I. Taylor's hypothesis according to which the space correlation depends only on spatial separation,[7,8,18] one can express the right hand side of Eq. (1), as a function of the correlation distance so that

$$R_{k\ell}(t_1,t_2) = g(r_{k\ell}) \tag{2a}$$

where

$$r_{k\ell} = [\{x_\ell(\bar{t}_2) - x_k(\bar{t}_1)\}^2 + \{y_\ell(\bar{t}_2) - y_k(\bar{t}_1)\}^2]^{1/2} \tag{2b}$$

Several analytical expressions are in use for $g(r_{k\ell})$. The preferred form of $g(r_{k\ell})$, which involves Bessel functions of fractional order, is due to von Karman. For low-altitude turbulence, typical of helicopter operations, the exponential autocorrelation function of vertical turbulence velocities provides a satisfactory approximation to the corresponding von Karman expression.[1] Following earlier works on rotor-gust models, we represent $g(r_{k\ell})$ by the exponential function

$$R_{k\ell}(r_{k\ell}) = \sigma_w^2 \{\exp(-2|r_{k\ell}|/L)\} \tag{3}$$

where σ_w is the standard deviation of the vertical turbulence velocity components, and L, the scale length of the longitudinal turbulence.

For a representative blade station, say station j, a distance r or c_jR from the rotor center, one has from Fig. 1,

$$dx_j(\bar{t})/d\bar{t} = v + r\Omega \sin\Omega\bar{t} = v + c_jR\Omega \sin\Omega\bar{t} \tag{4}$$

and

$$dy_j(\bar{t})/d\bar{t} = r\Omega\cos\Omega\bar{t} = c_jR\,\Omega\cos\Omega\,\bar{t} \tag{5}$$

where R is the rotor radius and c_j, a dimensionless constant.

Evaluating $x_\ell(\bar{t}_2)$, $y_k(\bar{t}_1)$, etc. from equations similar to Eqs. (4 and 5), the correlation distance $r_{k\ell}$ in Eq. (2b) reduces to

$$r_{k\ell} = [\{v(\bar{t}_2 - \bar{t}_1) - c_\ell R\cos\Omega\bar{t}_2 + c_kR\cos\Omega\bar{t}_1\}^2 + \{c_\ell R\sin\Omega\,\bar{t}_2 - c_kR\sin\Omega\,\bar{t}_1\}^2]^{1/2} \tag{6}$$

We now introduce a dimensionless time t such that the azimuth angle $\Omega\bar{t} = t$, and inflow ratio $\lambda = w/_{\Omega R}$, where w represents vertical turbulence velocities. With $\mu = v/_{\Omega R}$, where μ is the rotor advance ratio, and $a = 2\mu/(L/R)$, Eq. (3) can be expanded into

$$R_{k\ell}(t_1,t_2) = \sigma_\lambda^2 \exp(-|[\{a(t_2-t_1) - 2c_\ell(R/L)\cos t_2 + 2c_k(R/L)\cos t_1\}^2 + \{2c_\ell(R/L)\sin t_2 - 2c_k(R/L)\sin t_1\}^2]|^{1/2}) \tag{7a}$$

which can also be expressed in another form

$$R_{k\ell}(t_1,t_2) = \sigma_\lambda^2 \exp(-a|[\{(t_2-t_1) - (c_\ell/\mu)\cos t_2 + (c_k/\mu)\cos t_1\}^2 + \{(c_\ell/\mu)\sin t_2 - (c_k/\mu)\sin t_1\}^2]|^{1/2}) \tag{7b}$$

With $c_k = c_\ell$ one gets the autocorrelation function of vertical turbulence at blade station $c_\ell R$ from the rotor center.

For the case of uniform turbulence, one replaces Eqs. (4 and 5) by $dx_j/dt = \dot{x}_j = v$ and $\dot{y}_j = 0$. Therefore Eq. (7a) simplifies to the stationary model

$$R_{k\ell}(t_1,t_2) = \sigma_\lambda^2 \exp\{-a|t_2 - t_1|\} \tag{8a}$$

Taking the Fourier transform of both sides of Eq. (8a), we get the spectral density function

$$S_{k\ell}(\omega) = \sigma_\lambda^2 a/[\pi(a^2+\omega^2)] \tag{8b}$$

Such stationary random excitations can be simulated by passing the white noise u through the first-order filter under steady-state conditions

$$\dot{\lambda}_k = -a\lambda_k + \sigma_\lambda (2a)^{1/2} u \tag{9}$$

In this uniform turbulence model, the blade is assumed to encounter vertical turbulence velocities identical to that at the rotor center for all radial and azimuth positions. Therefore, the cross correlation function $R_{k\ell}(t_1,t_2)$ is also equal to the autocorrelation function $R_{kk}(t_1,t_2)$.

When nonuniformity is considered only in the flight direction, the right hand side of Eq. (5) is equal to zero and the correlation distance $r_{k\ell}$ is evaluated from Eq. (4). Therefore, Eq. (7a) simplifies to

$$R_{k\ell}(t_1,t_2) = \sigma_w^2 \exp\{-|a(t_2-t_1) - 2c_\ell(R/L)\cos t_2 + 2c_k(R/L)\cos t_1|\} \tag{10}$$

Setting $c_k = c_\ell = 0.7$, Eq. (10) reduces to the extended turbulence model developed by Gaonkar and Hohenemser, which represents the autocorrelation function of vertical turbulence at $0.7R$ blade station.[7,8] Similar to the simulation of stationary uniform turbulence by the shaping filter system in Eq. (9), the nonstationary turbulence given by Eq. (10) can also be simulated by the delay-type filter:

$$\lambda_k(t) = \hat{L}\,\lambda(t) = \lambda(t - c_k(R/L)\cos t) \tag{11}$$

where $\hat{L}$ is the operator of the linear delay-filter and $\lambda(t)$, the stationary turbulence input at the rotor center; for details see Sveshnikov.[21]

III. System Description

The analytical model describes the first flap-bending mode of a hingeless rotor blade in turbulence. Details of the flap-bending equations are given in Ref. 4, which also includes standard deviations of blade responses due to uniform gusts. The analysis is based on quasisteady linear aerodynamics including reversed flow, suitable for low rotor-lift and high ad-

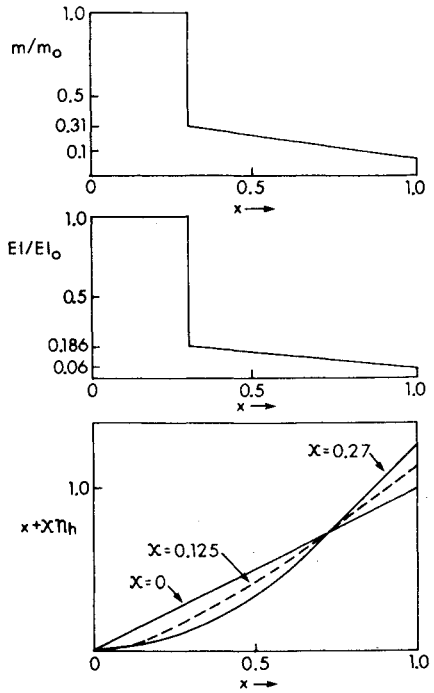

Fig.2 Mass, stiffness, and mode-shape profiles.

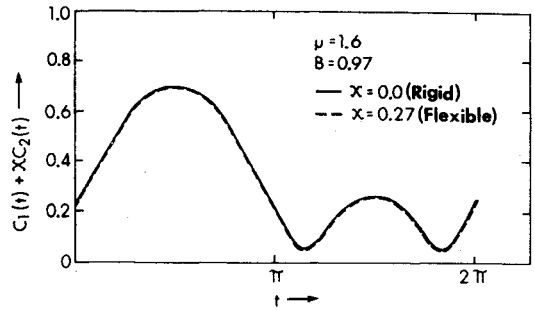

Fig. 3a Aerodynamic blade damping parameter for rigid flapping and first mode flap bending.

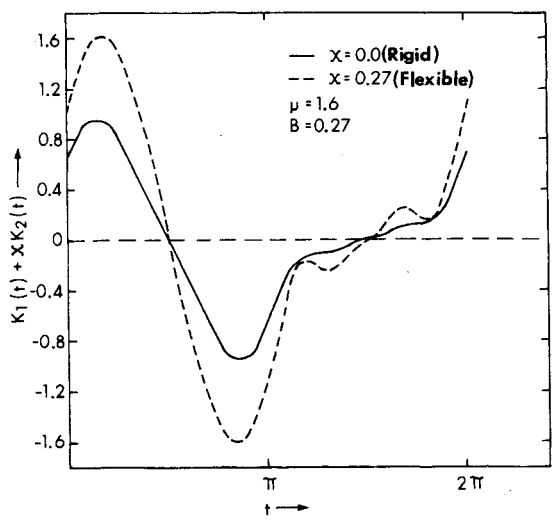

Fig. 3b. Aerodynamic blade stiffness parameter for rigid flapping and first mode flap bending.

vance ratio conditions. However, effects of nonuniform inflow, stall and compressibility and that of torsion or lead-lag coupling are neglected. These effects are expected to influence the low frequency flapping modes only to minor degree.[4]

Basically, an adaptation factor χ is introduced to represent the first elastic mode η in the form: $\eta = x + \chi\,\eta_h$, where η_h is the first elastic mode of a uniform hinged-free beam. With $\chi = 0$, one gets the rigid flapping or the straight line mode used by Sissingh.[20] When bending flexibility is included, χ is greater than zero. It is higher for a tapered-in-thickness blade than for the corresponding uniform blade. For example, as shown in Fig. 2, $\chi = 0.27$ for the nonuniform blade with flapping frequency $P = 1.47$, whereas $\chi = 0.125$ for the uniform blade with $P = 1.25$.[4] Figure 2 also shows the increased influence of flap-bending due to nonuniform mass and stiffness distribution.[4]

In a coordinate system which rotates with rotor angular velocity Ω, the linearized equation of blade flapping has the form (time unit $1/\Omega$):

$$\ddot{\beta} + (\gamma/2)[C_1(t) + \chi C_2(t)]\dot{\beta} + [p^2 + (\gamma/2)\{K_1(t) + \chi K_2(t)\}]\beta = (\gamma/2) m_\lambda(t)\lambda \tag{12}$$

The time variable functions in Eq. (12) are continuous periodic functions of period 2π having different Fourier expansions in the normal, mixed and reversed flow regions. Aerodynamic damping $C_1(t) + \chi C_2(t)$ and aerodynamic stiffness $K_1(t) + \chi K_2(t)$ are shown in Figs. 3a and 3b for $\chi = 0$ and 0.27 in combination with an advance ratio $\mu = 1.6$ and with a tip-loss factor $B = 0.97$. The input from the vertical turbulence is represented by $\lambda(t)$ in Eq. (12). As in earlier related studies, it is idealized at a representative blade station at $0.7R$ from the rotor center. Therefore, the input statistical description comprises only the scalar autocorrelation function which we represent by $R_\lambda(t_1, t_2)$. For the case of uniform turbulence, this autocorrelation function is given by Eq. (8a) which, as expected, is the same for all blade stations. For the other two cases 1) nonuniform only in the flight direction and 2) nonuniform over the entire rotor disk, $R_\lambda(t_1, t_2)$ is respectively given by Eqs. (10 and 7) with $c_k = c_\ell = 0.7R$. For subsequent discussion it is convenient to express Eq. (12) in matrix form. Therefore, with state variables β, $\dot{\beta}$, and $A(t)$ representing the 2×2 state or essential matrix, the flap-bending Eq. (12) can be expressed as

$$\dot{X} = \begin{Bmatrix} \beta \\ \dot{\beta} \end{Bmatrix}^{\bullet}$$

$$= \begin{bmatrix} 0 & 1 \\ -P^2 - \frac{\gamma}{2}\{K_1(t) + \chi K_2(t)\}, & -\frac{\gamma}{2}\{C_1(t) + \chi C_2(t)\} \end{bmatrix}$$

$$\times \begin{Bmatrix} \beta \\ \dot{\beta} \end{Bmatrix} + \begin{Bmatrix} 0 \\ \frac{\gamma}{2} m_\lambda(t) \end{Bmatrix} \lambda(t) \tag{13a}$$

Or in a compact form

$$\dot{X} = A(t)\,X + B(t)\lambda \tag{13b}$$

where $B(t)$ is the 2×1 column-matrix modulating the scalar random input function $\lambda(t)$.

IV. Response Variance

The three input models as typified by Eqs. (8, 10, and 7) have different stochastic features concerning filtering details and nonstationarity. Consequently, we have to adopt different methods of computing the response variance matrices. The following is a brief account of these methods:

For the case of uniform turbulence, the stationary correlation function is given by Eq. (8a), and the shaping filter system by Eq. (9). Combining the flapping Eq. (13b) with state variables β and $\dot{\beta}$, and the scalar filtering Eq. (9)

with the scalar state variable λ, we get the augmented or the combined system:

$$\begin{Bmatrix} X \\ \lambda \end{Bmatrix}^{\bullet} = \left[\begin{array}{c|c} A(t) & B(t) \\ \hline 0 & -a \end{array}\right] \begin{Bmatrix} X \\ \lambda \end{Bmatrix} + \begin{Bmatrix} \{o\} \\ \hline \sigma_w\sqrt{2a} \end{Bmatrix} u(t) \quad (14a)$$

With F as the 3×3 augmented state matrix corresponding to the 3×1 augmented state variable Y, Eq. (14a) takes the form

$$\dot{Y}=F(t)\,Y+Gu \quad (14b)$$

where G is the 3×1 augmented column matrix coupling the augmented state vector Y with the scalar white noise input $u(t)$. The variance matrix of Y denoted by $P(t)$, is defined by the relation $P(t)=E[Y(t)\,Y(t)^T]$, and is computed from the matrix differential equation

$$\dot{P}(t)=F(t)P(t)+P(t)F^T(t)+GG^T \quad (15)$$

under steady-state conditions.

When nonuniformity of the gust field is included over the entire rotor disk or only in the flight direction, the turbulence disturbances belong to a nonstationary random process, as seen from Eqs. (7 and 10). For nonstationary cases, the preceding approach according to Eq. (15) loses its computational simplicity, since it requires the synthesis of shaping filter systems with variable coefficients.[13] However, when the gust field is nonuniform only in flight direction, the input at any blade station can be simulated by passing the stationary random input at the rotor center through a delay-type filtering system indicated by Eq. (11). In other words, this input process characterized by Eqs. (10 and 11) can be treated as a modulated nonstationary process, in that a stationary process is modulated by a linear deterministic operation. Therefore, the response variance matrix can be evaluated from the equation

$$P(t)=\int_{-\infty}^{\infty} Y^*(\omega,t)s_\lambda(\omega)\,Y(\omega,t)^T\mathrm{d}\omega \quad (16)$$

where $s_\lambda(w)$ is the scalar spectral density function given by Eq. (8b). Computationally, Eq. (16) is identical to the conventional frequency response approach. However $Y(\omega,t)$ in Eq. (16) is the 2×1 response matrix to the delayed time input $\exp\{i\omega(t-(0.7/\mu)\cos t)\}$ or the solution of Eq. (13a) when $\lambda(t)$ is replaced by $Le^{i\omega t}$ as indicated in Eq. (11).

In the general case, when the gust field in the rotor disk is nonuniform both laterally and longitudinally, the nonstationary input correlation functions are given by Eq. (7a). Since this input process cannot be treated as a modulated nonstationary process the approach according to Eq. (16) is not applicable. An extended version of Eq. (16) to include nonstationary inputs involves two-dimensional integration and the double frequency Fourier transform of input correlation functions.[1] Therefore, for this general case, we follow the state transition matrix approach. As stated earlier, the inputs are idealized at $0.7R$ blade station and the input autocorrelation function $R_\lambda(t_1,t_2)$ is given by Eq. (7a) with $c_k=c_t=0.7R$.

For zero initial state, the state vector $X(t)$ with components β and $\dot{\beta}$ is governed by the dynamic Eq. (13a). If $\Phi(t,\theta)$ is the state transition matrix of this equation, the state vector $X(t)$ can be expressed as

$$X(t)=\int_0^t \Phi(t,\theta)B(\theta)\lambda(\theta)\mathrm{d}\theta \quad (17)$$

where $\Phi(t,\theta)$ is the solution of the matrix differential equation

$$\frac{\mathrm{d}}{\mathrm{d}t}\Phi(t,\theta)=A(t)\Phi(t,\theta);\ \Phi(\theta,\theta)=\begin{bmatrix}1&0\\0&1\end{bmatrix} \quad (18)$$

In Eq. (17) we need $\Phi(t,\theta)$ for variable θ, whereas the solution of Eq. (18) gives the state transition matrix for fixed θ and variable t. Computationally, it is often convenient to evaluate $\Phi(t,\theta)$ from the adjoint system equation

$$(\mathrm{d}/\mathrm{d}t)\Phi(t,\theta)=-A^T(\theta)\Phi(t,\theta) \quad (19)$$

with initial conditions

$$\Phi(t,t)=\begin{bmatrix}1&0\\0&1\end{bmatrix}$$

and with solution $\Phi(t,\theta)$ for a fixed t and variable θ. The state variance matrix or $E[X(t)X(t)^T]$ from Eq. (17) takes the form

$$P(t)=\int_0^t\int_0^t \Phi(t,\theta_1)B(\theta_1)E[\lambda(\theta_1)\lambda^T(\theta_2)]$$

$$B^T(\theta_2)\Phi^T(t,\theta_2)\mathrm{d}\theta_1\mathrm{d}\theta_2 \quad (20)$$

where $E[\lambda(\theta_1)\lambda(\theta_2)^T]$ is the input correlation function $R_\lambda(\theta_1,\theta_2)$ given by Eq. (7a). To minimize the area of integration we express the above equation in the form

$$P(t)=\int_0^t\int_0^\xi [\Phi(t,\theta_1)B(\theta_1)R_\lambda(\theta_1,\theta_2)B^T(\theta_2)\Phi^T(t,\theta_2)$$

$$+\Phi(t,\theta_2)B(\theta_2)R(\theta_2,\theta_1)B^T(\theta_1)\Phi^T(t,\theta_1)]\mathrm{d}\theta_1\mathrm{d}\theta_2 \quad (21)$$

where the expression inside the bracket [...] is symmetrical with respect to the diagonal line $\theta_1=\theta_2=\xi$. Equation (21) can be expressed as a series of one-dimensional integrations for which reliable computer techniques are available. In subsequent applications (Sec. VI) Eqs. (15, 16, and 21) are used respectively for uniform, partially nonuniform (nonuniform only in the longitudinal direction) and completely nonuniform turbulence inputs. For corresponding input covariance functions see Eqs. (8a, 10, and 7a).

V. Approximations to Peak Statistics

The basic formula in peak statistics concerns the average number of peaks (local maxima) per unit time above different vibration levels or thresholds. For example, with respect to flapping vibrations, it is given by[22]

$$E[M_\beta(\xi,t)]=-\int_\xi^\infty \mathrm{d}\beta\int_{-\infty}^0 \ddot{\beta}p_{\beta\dot{\beta}\ddot{\beta}}(\beta,\,0,\,\ddot{\beta},\,t)\mathrm{d}\ddot{\beta} \quad (22)$$

where $p_{\beta\dot{\beta}\ddot{\beta}}$ is the joint Gaussian probability density function between $\beta,\dot{\beta}$ and $\ddot{\beta}$. When threshold ξ in Eq. (22) tends to $-\infty$, we get $E[M_\beta(-\infty,t)]$ which gives the average number of peaks per unit time irrespective of magnitude or the average values of total peak rates. For simplicity of notation we represent $E[M_\beta(-\infty,t)]$ by $E[M_{\beta T}(t)]$. If there is a peak for blade azimuth position t, the probability that the height of this peak is less than or equal to ξ is given by the *distribution* function[15]

$$F_\beta(\xi,t)=1-\frac{E[M_\beta(\xi,t)]}{E[M_{\beta T}(t)]} \quad (23a)$$

The conditional probability *density* of peak magnitude or $p_\beta(\xi,t)$, and $F_\beta(\xi,t)$ are related by

$$F_\beta(\xi,t)=\int_{-\infty}^{\xi} p_\beta(\theta,t)\mathrm{d}\theta \quad (23b)$$

Several analytical expressions are used to approximate $F_\beta(\xi,t)$. The one credited to Powell[22] is based on the narrow-band approximations:

$$E[M_\beta(\xi,t)]\simeq E[N_{+\beta}(\xi,t)]$$

and

$$E[M_{\beta T}(t)] \simeq E[N_{+\beta}(0,t)] \tag{24}$$

where $E[N_{+\beta}(\xi,t)]$ is the average of the random rate at which the response component β crosses the vibration level ξ from below or with positive slope. Closed form expressions of

$$E[M_{\beta T}(t)],\ E[N_{+\beta}(\xi,t)],\ \frac{\partial}{\partial \xi} E[N_{+\beta}(\xi,t)]$$

and $p_{\beta}(\xi,t)$ are given in Ref. 15. For example $E[N_{+\beta}(\xi,t)]$, can be expressed as [1]

$$E[N_{+\beta}(\xi,t)] = \sigma_{\dot\beta}(2\pi\sigma_{\beta})^{-1}(1-r^2_{\beta\dot\beta})^{1/2} \times \exp(-\xi^2/2\sigma^2_{\beta})[\exp(-\nu^2)+\pi^{1/2}\nu(1+\operatorname{erf}\nu)] \tag{25}$$

where σ_{β} and $\sigma_{\dot\beta}$ are the root mean square values or $\sqrt{R_{\beta\beta}}$ and $\sqrt{R_{\dot\beta\dot\beta}}$, respectively. Further, the error function erfν, the correlation coefficient $r_{\beta\dot\beta}$ and ν are given by

$$\operatorname{erf}(\theta) = \frac{2}{(\pi)^{1/2}} \int_0^{\theta} e^{-t^2} dt \qquad r_{\beta\dot\beta} = \frac{R_{\beta\dot\beta}}{\sigma_{\beta}\sigma_{\dot\beta}}$$

and

$$\nu = (\xi/\sigma_{\beta}) r_{\beta\dot\beta}[2(1-r^2_{\beta\dot\beta})]^{-1/2}$$

It is instructive to observe that $E[N_{+\beta}(\xi,t)]$ depends on $R_{\beta\dot\beta}(t)$, $R_{\dot\beta\dot\beta}(t)$ and $R_{\ddot\beta\dot\beta}(t)$, which are the three elements of the symmetrical response variance matrix between β and $\dot\beta$ discussed earlier. The evaluation of $E[M_{\beta T}(t)]$ is relatively more elaborate,[15] since it requires the six elements of the symmetric variance matrix between β, $\dot\beta$ and $\ddot\beta$. In the present paper $E[M_{\beta T}(t)]$ is computed from the closed form expression given in Ref. 15, whereas $E[M_{\beta}(\xi,t)]$ is evaluated by reducing the right hand side of Eq. (22) into one-dimensional integration, and then computing the final one-dimensional quadrature with limits ξ and ∞ numerically.

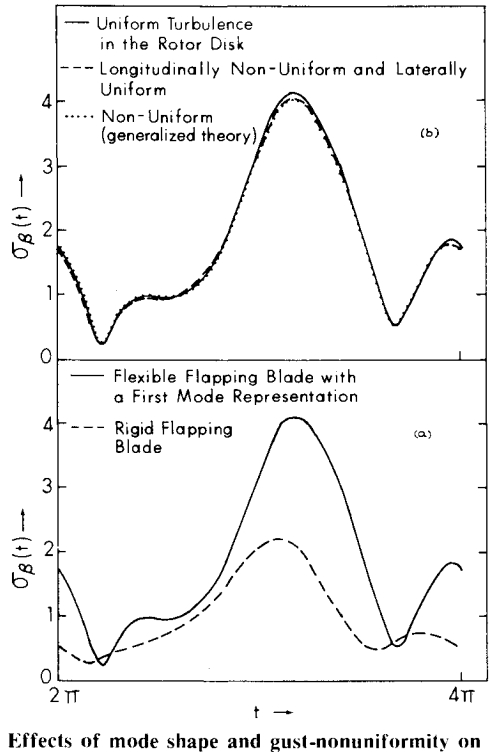

Fig. 4 Effects of mode shape and gust-nonuniformity on response standard deviations.

While studying certain narrow-band features of the rotor response process, it is convenient to introduce a parameter $\rho_{\beta}(\xi)$ as the ratio between the total number of peaks above ξ, and the total number of threshold upcrossings of ξ in one rotor revolution

$$\rho_{\beta}(\xi) = \frac{\int_0^{2\pi} E[M_{\beta}(\xi,t)]dt}{\int_0^{2\pi} E[N_{+\beta}(\xi,t)]dt} \tag{26}$$

where 2π is the period of the response process after time unit normalization. The rotor response to gust is a weakly periodic nonstationary process with period equal to 2π or the time of one rotor revolution.[13] The mean and the variance of such a process are invariant, not for arbitrary time shifts as in a stationary process, but under a time shift of an integral multiple of the period. It is therefore of interest to study the peak distribution over one rotor revolution which is independent of instantaneous blade azimuth locations and which leads to a simpler equation than Eq. (23a). We define the peak distribution function of β over one rotor revolution as follows [14,16]

$$F_{\beta T}(\xi) = \text{Prob}\{\text{any maxima of } \beta \le \xi \text{ in one rotor revolution}\}$$
$$= 1 - \{\int_0^{2\pi} E[M_{\beta}(\xi,t)]dt / \int_0^{2\pi} E[M_{\beta T}(t)]dt\} \tag{27}$$

In the process of reconciling Eq. (27) with Eq. (23a), we express $F_{\beta T}(\xi)$ in Eq. (27) as follows

$$F_{\beta T}(\xi) = \frac{\int_0^{2\pi} F_{\beta}(\xi,t) E[M_{\beta T}(t)]dt}{\int_0^{2\pi} E[M_{\beta T}(t)]dt} \tag{28}$$

Here we have replaced $E[M_{\beta}(\xi,t)]$ in Eq. (27) using Eq. (23a). Since $F_{\beta}(\xi,t)$ and $E[M_{\beta T}(t)]$ are continuous and since $E[M_{\dot\beta T}(t)] > 0 (0 \le t \le 2\pi)$, we invoke the mean value theorem to obtain

$$F_{\beta T}(\xi) = F_{\beta}(\xi,\bar t),\ 0 < \bar t < 2\pi \tag{29}$$

Equation (29) thus demonstrates that $F_{\beta T}(\xi)$ is the weighted arithmetic average of $F_{\beta}(\xi,t)$ in one rotor revolution with respect to the weighting function $E[M_{\beta T}(t)]$. Finally, we study the following approximations

$$\int_0^{2\pi} E[M_{\beta}(\xi,t)]dt \simeq \int_0^{2\pi} E[N_{+\beta}(\xi,t)]dt$$

and

$$\int_0^{2\pi} E[M_{\beta T}(t)]dt \simeq \int_0^{2\pi} E[N_{+\beta}(0,t)]dt \tag{30}$$

which significantly simplify the computation of $F_{\beta T}(\xi)$ in Eq. (27).

VI. Discussion of Results

All the graphically illustrated numerical results are for the following system parameters: advance ratio $\mu = 1.6$, tip-loss factor $B = 0.97$, angular rotor speed $\Omega = 1$, Lock inertia number $\gamma = 5$, and the flapping frequency $p = 1.47$. For the vertical-gust, the ratio of turbulence scale length L over the rotor radius R is equal to 12 and, the standard deviation $\sigma_{\lambda} = 1$. Only the time interval during second rotor revolution ($2\pi \le t \le 4\pi$) is selected when the system is under steady-state con-

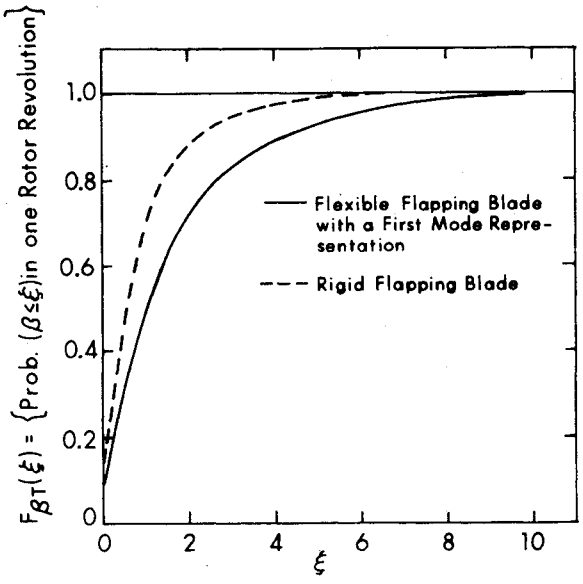

Fig. 5 Response peak distribution functions over one rotor revolution for rigid and flexible blade.

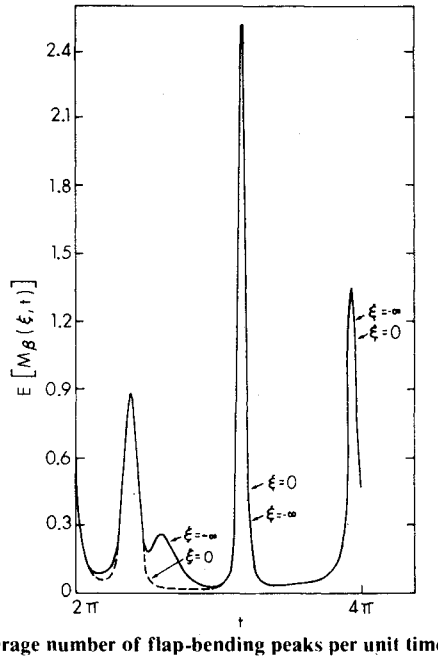

Fig. 6 Average number of flap-bending peaks per unit time irrespective of magnitude and above zero mean level.

ditions, and when the system response belongs to a (weakly) periodic nonstationary process. Unless stated otherwise, the results refer only to flap bending with $\chi = 0.27$, where χ is the adaptation factor for the first mode representation of the tapered-in-thickness blade shown in Fig. 2. For the same blade, aerodynamic stiffness and damping functions are shown in Figs. 3a and 3b. In Fig. 4a, the response standard deviations of a flap bending blade ($\chi = 0.27$) are compared with that of a rigid flapping blade ($\chi = 0.0$) for uniform (stationary) turbulence. The input correlation function is given by Eq. (8a), and the shaping filter, by Eq. (9). The response standard deviations are computed according to the shaping filter method typified by Eq. (15). The inclusion of the first elastic mode almost doubles the absolute maximum of $\sigma_\beta(t)$ in one rotor evolution.

In Fig. 4b, the standard deviations of flap bending are presented for three cases of turbulence inputs which are also identified in the same figure. The case of uniform turbulence is the same as that presented in Fig. 4a for the flexible blade.

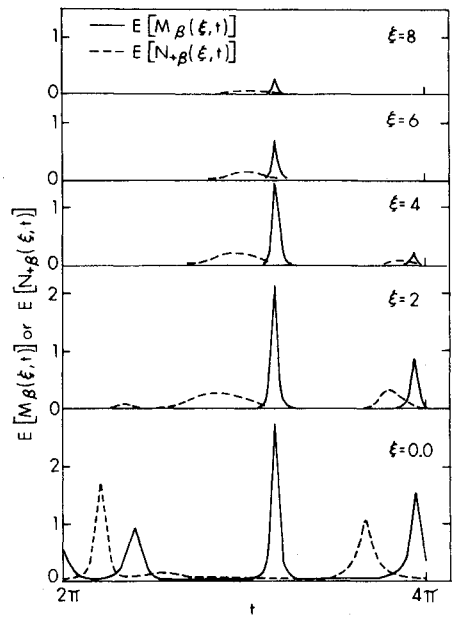

Fig. 7 Average number of peaks and threshold upcrossing per unit time for different response levels.

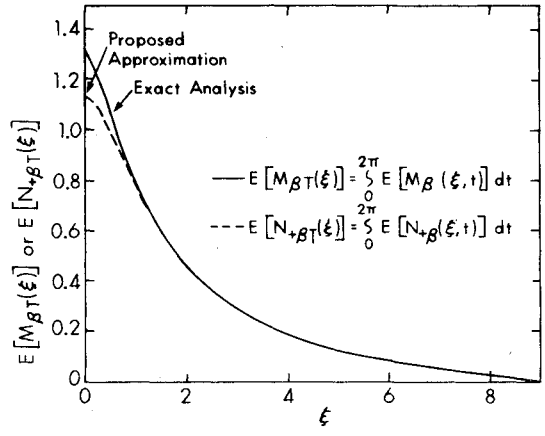

Fig. 8 Narrow-band features of the response process over one rotor revolution, Eqs. (26) and (30).

For both nonuniform and partially nonuniform turbulence, scalar input autocorrelation functions for a representative blade station at 0.7 radius are respectively given by Eqs. (7 and 10) with $C_k = C_\ell = 0.7$. For the nonuniform case, $\sigma_\beta(t)$ is computed from Eq. (21); whereas for the partially nonuniform case, from Eqs. (16 and 8b). As we observe from Fig. 4b, the uniform turbulence model is an excellent approximation to the two nonuniform cases, and it provides slightly conservative results with respect to the absolute maximum of $\sigma_\beta(t)$. In order to further substantiate this observation, we reduced L/R from 12 to 4 for the same three input models and computed $\sigma_\beta(t)$ of the flap-bending blade for a few typical azimuth locations. When compared to the two nonuniform models according to Eqs. (7 and 10), the uniform turbulence model is conservative and the error is well within 15%. This means that computing the response variance matrix and related threshold crossing expectations essentially reduces to solving a linear matrix differential equation, Eqs. (15) and (25). Since the influence of nonuniformity of vertical turbulence in the rotor plane is negligible, the rest of the numerical results presented in Figs. 5 to 9 are based on the uniform turbulence model.

Figure 5 shows the probability of flapping excursions in one rotor revolution according to Eq. (27). It is seen that $\beta(t)$ could reach values as high as $2.5\sigma_{\beta\max}$ with a probability of

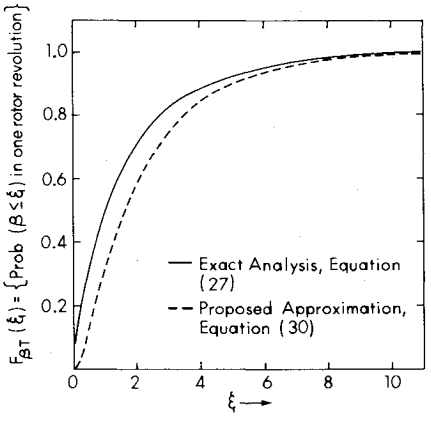

Fig. 9 Narrow-band approximation to response peak distribution over one rotor revolution.

approximately 0.05 for both rigid and elastic blades, where $\sigma_{\beta\max}$ is the corresponding absolute maximum of $\sigma_\beta(t)$ in one rotor revolution. From Fig. 4a we have $\sigma_{\beta\max} \simeq 2$ for the rigid blade and $\sigma_{\beta\max} \simeq 4$ for the flap-bending blade. The results in Fig. 5 thus demonstrate that, for the same gust excitation, the vibration levels are about 2.5 times higher for the elastic blade than those for the rigid blade. Thus the inclusion of flap bending, as required in the simulation of a hingeless rotorcraft, significantly increases the vibration levels due to gust encounter.

In Figs. 6, 7, and 8, we study the narrow-band features of rotor responses which belong to a weakly periodic nonstationary process. The period of the response process is equal to the period of one rotor revolution. In this study, the rotor response is said to be narrow-band, above threshold ξ, and during one rotor revolution if $\rho(\xi)$ in Eq. (26) is equal to one. For a periodic nonstationary process, irrespective of its narrow-band features, the average of the total number of peaks above ξ in one period is always equal to or greater than the average of the total number of threshold upcrossings of ξ during the same period. Therefore $\rho(\xi) = 1$ in Eq. (26) reveals an inherent structure of narrow-band features, i.e., one and only one peak above ξ is followed by one upcrossing of ξ. For example, if a process having zero mean values is narrow band for all thresholds, then all the (total) peaks will be above the zero mean level, and all the troughs (local minima) below this level. We also observe in passing that for a stationary process $E[M_\beta(\xi,t)]$ and $E[N_{+\beta}(\xi,t)]$ are time invariant. Therefore $\rho(\xi) = 1$ and Powell's approximation according to Eq. (24) are equivalent to each other. However for periodic nonstationary processes $\rho(\xi) = 1$ does not necessarily imply Powell's approximation, whereas Powell's approximation implies $\rho(\xi) = 1$ in Eq. (26). Thus Powell's approximation for nonstationary processes involves a more stringent restriction than is involved in Eq. (26).

As outlined earlier, all the peaks occur above the zero threshold for a zero-mean narrow-band process. Therefore in Fig. 6, we study the two types of peaks per unit time – peaks irrespective of magnitude, and peaks above the zero-mean level of the response process. The total number of peaks irrespective of magnitude is obtained by integrating the area under the curve of $E[M_{\beta T}(t)]$ from 2π to 4π. It is about 20% higher than the total number of peaks above the mean level. Thus the flap-bending response deviates only 'slightly' from being a narrow-band process. At this stage two questions arise: 1) what is the range of threshold levels within which the response process deviates from being a narrow-band process? and 2) how far is it feasible to approximate the peak statistics by corresponding threshold crossing statistics as typified by Eqs. (24 and 30)? These questions are explored in Figs. 7, 8 and 9.

Figure 7 shows that Powell's widely used narrow-band approximations according to Eq. (24) are not satisfactory for all threshold ranges including high response levels ($\xi > \sigma_{\beta\max}$), whereas Fig. 8 shows that the "averaged" narrow-band approximations according to Eq. (30) are satisfactory for high response levels. From Fig. 4 we have $\sigma_{\beta\max}$ close to 4. It is seen from Fig. 8 that $\rho_\beta(\xi)$ defined in Eq. (26) is approximately equal to 1 for $\xi \ge 0.5\sigma_{\beta\max}$, thus demonstrating that the response process is narrow band over one rotor revolution for $\xi \ge 0.5\sigma_{\beta\max}$. Of particular importance in reliability studies is the probability of high level excursions in one rotor revolution. Therefore we computed $F_{\beta T}(\xi)$, defined in Eq. (27), using the narrow-band approximations according to Eq.. (30). As shown in Fig. 9, the proposed approximation according to Eq. (30) is satisfactory for $\xi \ge \sigma_{\beta\max}$. Although the response process is narrow-band for $\xi \ge 0.5\sigma_{\beta\max}$, the proposed approximations to compute $F_{\beta T}(\xi)$ are satisfactory for $\xi \ge \sigma_{\beta\max}$. Observe that we have to approximate both

$$\int_0^{2\pi} E[M_\beta(\xi,t)]\mathrm{d}t \quad \text{and} \quad \int_0^{2\pi} E[M_{\beta T}(t)]\mathrm{d}t$$

in Eq. (27) by the corresponding threshold crossing approximations given by Eq. (30).

VII. Conclusion

This exploratory study based on the first mode flap-bending analysis of uniform and tapered-in-thickness flapwise stiff blades subject to vertical gust excitations during low rotor-lift and high advance ratio operations and neglecting induced flow but including reversed flow leads to the following conclusions.

1) The effects of nonuniformity of turbulence in the lateral and flight directions of the rotor disk are negligible. In other words, the stationary atmospheric turbulence as it exists at the rotor center is the representative sample for the entire rotor disk. This finding is of particular significance for the further development of the stochastic treatment of lifting rotors, particularly in the development of test procedures to measure input data.

2) The peak distribution analysis shows that the probability that flap-bending and rigid flapping peaks can reach values as high as $2.5\sigma_{\beta\max}$, is close to 0.05, where $\sigma_{\beta\max}$ is the respective absolute maximum of $\sigma_\beta(t)$ in one rotor revolution.

3) The flap-bending response process is narrow band in that $\rho_\beta(\xi)$ defined in Eq. (26) is equal to 1 for $\xi \ge 0.5\sigma_{\beta\max}$.

4) Powell's approximations as typified by Eq. (24) are not satisfactory for any threshold ranges and azimuth positions. This observation can be treated as an extended version of an earlier study[15] in which it is shown that $(\partial/\partial\xi)E[M_\beta(\xi,t)]$ cannot be approximated by $(\partial/\partial\xi)E[N_{+\beta}(\xi,t)]$ for rigid flapping responses. (Computationally $(\partial/\partial\xi)E[M_\beta(\xi,t)]$ is simpler to evaluate than $E[M_\beta(\xi,t)]$.)

5) The probability that the flap-bending excursions in one rotor revolution are less than or equal to a preset response level ξ, can be approximated by using the averaged narrow-band approximations according to Eq. (30) for $\xi \ge \sigma_{\beta\max}$. This means that the complete response statistics of applied interest,[22] i.e., root mean square values, threshold crossing and high level peak statistics, can be obtained essentially by solving a differential equation similar to the original equations of motion [see Eqs. (15, 25, and 30)].

Acknowledgments

The author would like to thank E. Jason, L. Lockett, and N. Wallace, Southern Illinois University, for encouragement, and K. H. Hohenemser, Washington University, St. Louis, for discussions and comments. This research was supported by the Office of the Assistant Vice President for Special Programs and Minority Affairs and by the Office of Research and Projects, Southern Illinois University, Edwardsville.

References

[1]Caonkar, G. H. and Hohenemser, K. H., "Stochastic Properties of Turbulence Excited Rotor Blade Vibrations," *AIAA Journal*, Vol. 9, March 1971, pp. 419-421.

[2]Gaonkar, G. H., Hohenemser, K. H., and Yin, S. K., "Random Gust Response Statistics for Coupled Torsion-Flapping Rotor Blade Vibrations," *Journal of Aircraft*, Vol. 9, Oct. 1972, pp. 726-729.

[3]Kana, D. D. and Chu, W. H., "The Response of a Model Helicopter Rotor Blade to Random Excitation During Forward Flight," Southwest Research Institute, San Antonio, Houston, Final Report, Contract No. DA-31-124-AROD-375, U.S. Army Research Office, Durham, N.C., Aug. 1972.

[4]Hohenemser, K. H. and Yin, S. K., "On the Question of Adequate Hingeless Rotor Modeling in Flight Dynamics," preprint 732, 29th Annual National Forum of the American Helicopter Society, Washington, D.C., May 1973.

[5]Hohenemser, K. H. and Yin, S. K., "On the Use of First Order Rotor Dynamics in Multiblade Coordinates," preprint 743, 30th National Forum of the American Helicopter Society, Washington, D.C., May 1974.

[6]Peters, D. A., "Hingeless Rotor Frequency Response with Unsteady Inflow," *Proceedings of the Specialists Meeting on Rotorcraft Dynamics*, NASA/American Helicopter Society, Moffett Field, Calif., Feb. 1974, pp. 1-12.

[7]Gaonkar, G. H. and Hohenemser, K. H., "Comparison of Two Stochastic Models for Threshold Crossing Studies of Rotor Blade Vibrations," AIAA Paper 71-389, Anaheim, Calif., 1971.

[8]Gaonkar, G. H and Hohenemser, K. H., "An Advanced Stochastic Model for Threshold Crossing Studies of Rotor Blade Vibrations," *AIAA Journal*, Vol. 10, Aug. 1972, pp. 1100-1101.

[9]Wan, F. Y. M. and Lakshmikantham, C., "Spatial Correlation Method and a Time-Varying Flexible Structure," *AIAA Journal*, Vol. 12, May 1974, pp. 700-707.

[10]Wan, F. Y. M., "Effect of Spanwise Load-correlation on Rotor Blade Flapping," AIAA Paper 74-418, Las Vegas, Nev., 1974.

[11]Wan, F. Y. M., "A Direct Method for Linear Dynamical Problems in Continuum Mechanics with Random Loading," *Studies in Applied Mathematics*, Vol. 52, 1973, pp. 259-275.

[12]Appa Rao, T. A. P. S., "An Experimental and Theoretical Investigation of Propellers Operating in Turbulence," Institute for Aerospace Studies, University of Toronto, Toronto, Can., UTIAS Rept. No. 183, Nov. 1972.

[13]Gaonkar, G. H., "A General Method with Shaping Filters to Study Random Vibration Statistics of Lifting Rotors with Feedback Controls," *Journal of Sound and Vibration*, Vol. 21, 1972, pp. 213-225.

[14]Shinozuka, M. and Yank, J. N., "Peak Structural Response to Nonstationary Random Excitation," *Journal of Sound and Vibration*, Vol. 16, 1971, pp. 505-517.

[15]Gaonkar, G. H., "A Study of Rotor Flapping Response Peak Distribution in Atmospheric Turbulence," *Journal of Aircraft*, Vol. 11, Feb. 1974, pp. 104-111.

[16]Gaonkar, G. H., "Peak Statistics and Narrow-band Features of Coupled Torsion-Flapping Rotor Blade Vibrations to Turbulence," *Journal of Sound and Vibration*, Vol. 34, 1974, pp. 35-52.

[17]Barlow, J. B., Theory of Propeller Forces in a Turbulent Atmosphere, Ph.D. Thesis, Institute for Aerospace Studies, University of Toronto, Toronto, Can., May 1970.

[18]Taylor, J., *Manual on Aircraft Loads*, AGARDograph 83, Ch. 10, Pergamon Press, New York, 1965.

[19]Gault, J. D. and Gunter, D. E., "Atmospheric Turbulence Considerations for Future Aircraft Designed to Operate at Low Altitudes," *Journal of Aircraft*, Vol. 5, Nov. 1968, pp. 574-577.

[20]Sissingh, G. J., "Dynamics of Rotors Operating at High Advance Ratios," *Journal of American Helicopter Society*, Vol. 17, July 1972, pp. 56-63.

[21]Sveshnikov, A. A., "Applied Methods of the Theory of Random Functions," Ch. 2, Pergamon Press, New York, 1966.

[22]Lin, Y. K., *Probabilistic Theory of Structural Dynamics*, Ch. 9, McGraw-Hill, New York, 1967.

From the AIAA Progress in Astronautics and Aeronautics Series . . .

AEROACOUSTICS: FAN, STOL, AND BOUNDARY LAYER NOISE; SONIC BOOM; AEROACOUSTIC INSTRUMENTATION—v. 38

Edited by Henry T. Nagamatsu, General Electric Research and Development Center; Jack V. O'Keefe, The Boeing Company; and Ira R. Schwartz, NASA Ames Development Center
A companion to Aeroacoustics: Jet and Combustion Noise; Duct Acoustics, volume 37 in the series.

Twenty-nine papers, with summaries of panel discussions, comprise this volume, covering fan noise, STOL and rotor noise, acoustics of boundary layers and structural response, broadband noise generation, airfoil-wake interactions, blade spacing, supersonic fans, and inlet geometry. Studies of STOL and rotor noise cover mechanisms and prediction, suppression, spectral trends, and an engine-over-the-wing concept. Structural phenomena include panel response, high-temperature fatigue, and reentry vehicle loads, and boundary layer studies examine attached and separated turbulent pressure fluctuations, supersonic and hypersonic.

Sonic boom studies examine high-altitude overpressure, space shuttle boom, a low-boom supersonic transport, shock wave distortion, nonlinear acoustics, and far-field effects. Instrumentation includes directional microphone, jet flow source location, various sensors, shear flow measurement, laser velocimeters, and comparisons of wind tunnel and flight test data.

509 pp. 6 x 9, illus. $19.00 Mem. $30.00 List

TO ORDER WRITE: Publications Dept., AIAA, 1290 Avenue of the Americas, New York, N. Y. 10019